

Synthesis and characterization of new thiophene–benzimidazole-based electrochromes

Emine Gül CANSU ERGÜN*

Department of Electrical and Electronics Engineering, Faculty of Engineering, Başkent University, Ankara, Turkey

Received: 10.10.2017

Accepted/Published Online: 08.01.2018

Final Version: 27.04.2018

Abstract: In the present study, two new donor–acceptor–donor-type molecules were synthesized and the electro-optical properties of the resulting monomers and their corresponding polymers were investigated. Thiophene was selected as the donor unit and cycloheptyl- and cyclooctyl- substituted benzimidazoles were used as the acceptor units. The synthesized monomers and their electrochemically obtained polymers were characterized using cyclic voltammetry and UV-Vis spectrometry. The optical band gap values of the polymers were 1.62 eV and the polymer films changed color to gray upon oxidation, while they were brick red in their neutral states. Moreover, changing the ring size on the acceptor group from seven carbon to eight carbon did not result in any differences in the electrochemical or optical properties of the resulting polymers. Moreover, the effect of the acceptor unit was also investigated by comparing the polymers in this work with other polymers bearing thiophene and benzimidazole.

Key words: Thiophene, benzimidazole, electrochemical polymerization, conjugated polymers, donor-acceptor approach

1. Introduction

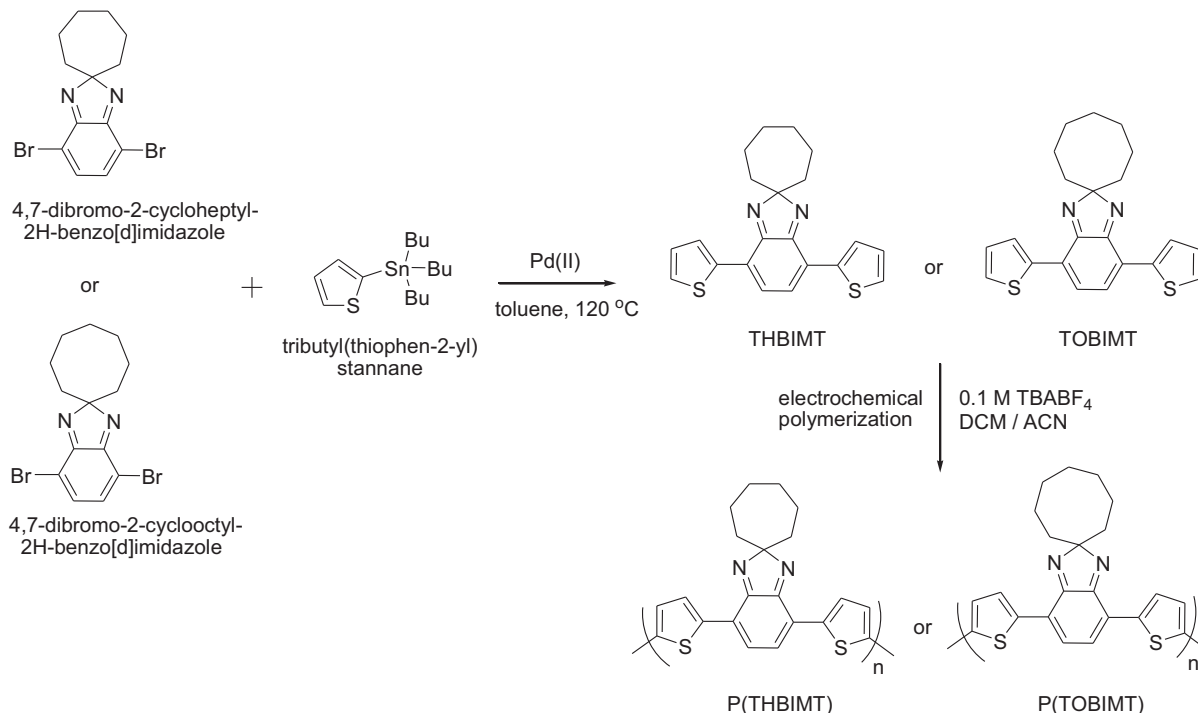
Donor–acceptor–donor type (DAD) conjugated polymers (CPs) are of great interest due to their enhanced electro-optical properties.^{1–3} Combination of an electron-deficient molecule with an electron-rich one allows intramolecular charge transfer (ICT) occurring from the donor unit to the acceptor molecule, resulting in an increase in the conjugation and a red-shifted optical absorption of the resulting monomers and polymers. Moreover, the optical, electrochemical, and thermal properties can be altered by changing the donor and the acceptor groups in the monomer structure.^{4–6} Modifying the molecular structure can also cause solubility in the corresponding polymers, which makes them processable.^{7,8} CPs have been used in many fields such as organic light emitting diodes,^{9,10} smart windows,¹¹ organic solar cells,^{12–14} field effect transistors,¹⁵ screens,¹⁶ and camouflage materials,¹⁷ as well as in biosensing applications.¹⁸

Various types of donor and acceptor groups have been designed and synthesized in the literature so far. Commonly used acceptor groups in conjugated polymer synthesis are benzazoles.^{19–21} Although the mostly commonly used acceptor unit among benzazoles is benzothiadiazole,^{22,24} benzimidazole (BIM) has also attracted attention due to its ability of functionalization from its 2C position; thus, various BIM derivatives can be designed by each different substitution, showing different behaviors. For example, since most of the benzazoles cannot be substituted, alkyl substitutions are commonly used on the donor units for achieving solubility. However, alkyl-substituted BIM is a good candidate as an acceptor unit that can cause solubility in

*Correspondence: egulcansu@baskent.edu.tr

the resulting polymers without disturbing the planarity of the chain.^{25,26} Furthermore, changing both hydrogens on the 2C position of the BIM unit with cyclic or aromatic groups can cause a significant decrease in the optical band gap of the resulting polymers.^{27–29}

In the present study, thiophene and cycloheptyl- and cyclooctyl-substituted benzimidazoles were selected as the donor and the acceptor groups, respectively. After synthesis and the characterization of the monomers, polymer films were obtained via electrochemical techniques (Scheme). The electrochemical and optical properties of two monomers and their corresponding polymers were compared in terms of the ring size on the acceptor unit.



Scheme. Synthesis route to monomers and their corresponding polymers.

2. Results and discussion

2.1. Electrochemical and optical properties of the monomers

To investigate the electrochemical and behavior of the monomers, cyclic voltammograms (CVs) were collected. For CVs, monomer solution was prepared in an ACN/DCM mixture (90:10 vol/vol) by adding TBABF₄ as a supporting electrolyte. The ACN/DCM solvent mixture was used since the monomers have weak solubility in ACN. The CVs were obtained by applying potentials between 0.0 V and 1.2 V on a Pt disc. During the anodic scan, both **THBIMT** and **TOBIMT** gave an irreversible oxidation peak that starts at about 0.90 V (oxidation onset potential) and reaches its maximum at 1.02 V (Figure 1).

In order to observe the optical behavior, UV-Vis and fluorescence spectra of the monomers were measured in DCM and the resulting spectra are shown in Figure 2. Both monomers gave a dual absorption band with two maximum peaks at 300 nm and 487 nm, due to its donor-acceptor pattern (Figure 2a). The former band can be assigned to $\pi-\pi^*$ transition, whereas the lowest energy band is due to the ICT between the donor (thiophene)

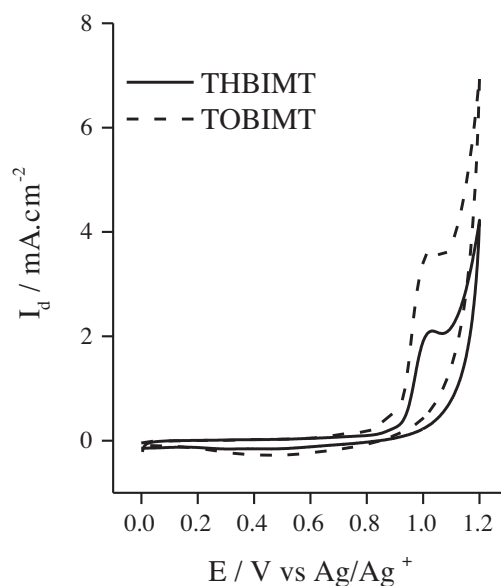


Figure 1. Cyclic voltammograms of **THBIMT** and **TOBIMT** monomers in 0.1 M TBABF₄/ACN-DCM (90:10) electrolytic solution (between 0.0 V and 1.2 V at a scan rate of 100 mV/s).

and the acceptor (BIM) moieties.³⁰ Moreover, the maximum of the emission band for both monomers was at 608 nm in DCM (Figure 2b).

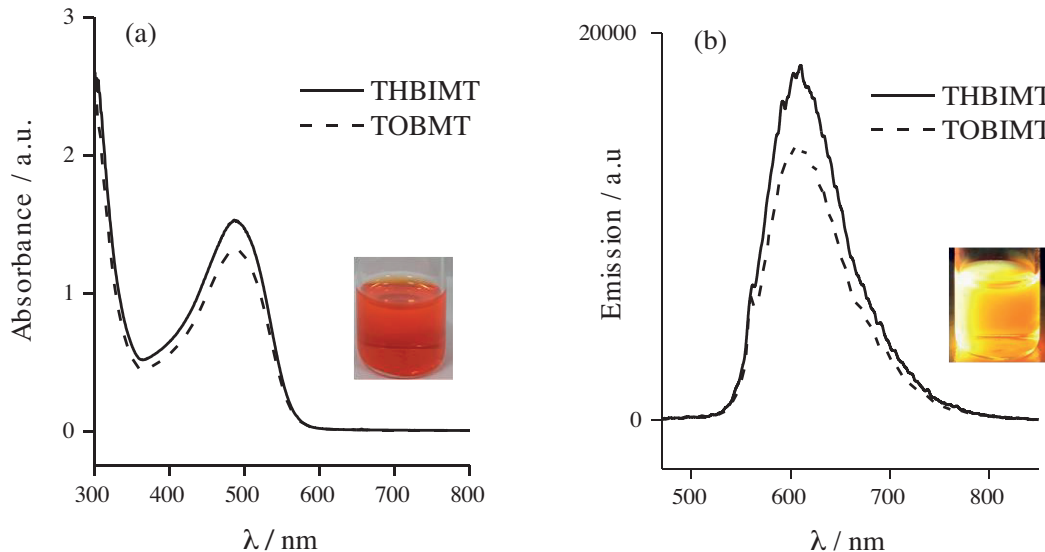


Figure 2. a) UV-Vis and b) Emission spectra of **THBIMT** and **TOBIMT** monomers in DCM. Insets: Color of the monomers under daylight (a) and UV light (b).

2.2. Electrochemical and optical properties of the polymers

The polymer films were obtained electrochemically on a Pt disc electrode via potential cycling by applying potentials between 0 and 1.1 V (Figure 3). During polymerization, a new reversible redox couple appeared at around 0.5 V, along with the original monomer oxidation at 1.02 V, for both polymerizations (Figures 3a and

3b). The intensity of the peaks increased in each successive scan, showing progressive polymer formation on the working electrode surface. After 15 cycles, the resulting polymer films were washed in ACN/DCM and placed into monomer free electrolytic medium (0.1 M TBABF₄ in ACN). Figure 3c shows the CVs of the polymer films during the anodic and cathodic scans. The onset of the oxidation potentials were 0.45 V, reaching a maximum at 0.92 V for both **P(THBIMT)** and **P(TOBIMT)**. The polymer films did not reveal any electrochemical behavior during scanning at negative potentials in TBABF₄/ACN.

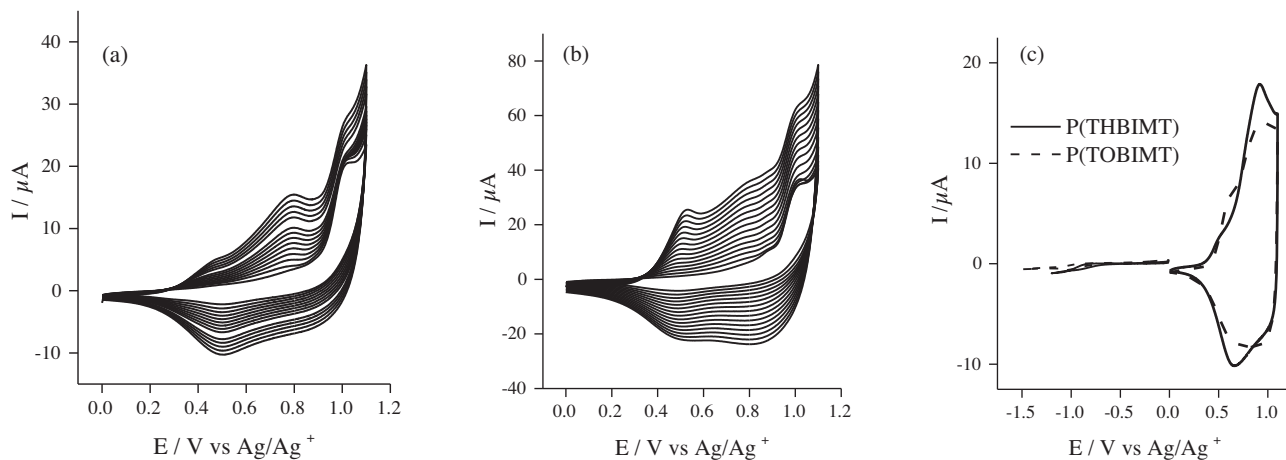


Figure 3. Electro-polymerization of a) **THBIMT** and b) **TOBIMT** in 0.1 M TBABF₄/ACN-DCM (90:10) electrolytic solution (15 scans between 0.0 V and 1.2 V at a scan rate of 100 mV/s), c) CV of the resulting polymer films, **P(THBIMT)** and **P(TOBIMT)**, in 0.1 M TBABF₄/ACN monomer-free electrolytic solution at a scan rate of 100 mV/s.

The long-term stability of a polymer film upon many switches is an important parameter for electrochromic applications. In order to test the electrochemical stability, polymer films (on a Pt disc electrode) were switched between their neutral and oxidized states under square wave input of 0.0 V and 1.1 V in 3-s intervals. After 500 redox cycle, 62% and 55% of cathodic and 56% and 58% of anodic current loss were observed in electro-activity of **P(THBIMT)** and **P(TOBIMT)**, respectively, indicating poor electrochemical stability upon many fast switches. The reason for this large current loss is obviously the high oxidation potential (1.1 V) that we applied to the polymer films.

Scan rate dependence of the polymers is also an important parameter to understand if the redox process is effective even upon short switching times. For this reason, CVs of **P(THBIMT)** and **P(TOBIMT)** were collected upon increasing scan rates between 40 mV/s and 200 mV/s with 40-mV increments (Figure 4). As seen from Figures 4a and 4b, the scan rate dependence of both polymer films showed good linearity for the anodic and cathodic current change upon increasing the scan rate (see insets of Figures 4a and 4b). It can be concluded that **P(THBIMT)** and **P(TOBIMT)** reveal a nondiffusional redox process and both polymer films are well adhered on the working electrode surface.

In order to monitor the change in the electronic absorption spectrum upon oxidation, the polymer films were obtained on an ITO-glass electrode via constant potential electrolysis. Then UV-Vis spectra were collected during the anodic scans of the resulting films from -0.2 V to 1.2 V vs. Ag wire at a scan rate of 20 mV/s (Figure 5). As seen from Figure 5a, **P(THBIMT)** exhibited two absorption bands, the first band as a shoulder with a maximum at 360 nm and the second having a maximum at 504 nm. In the same way, **P(TOBIMT)** exhibited

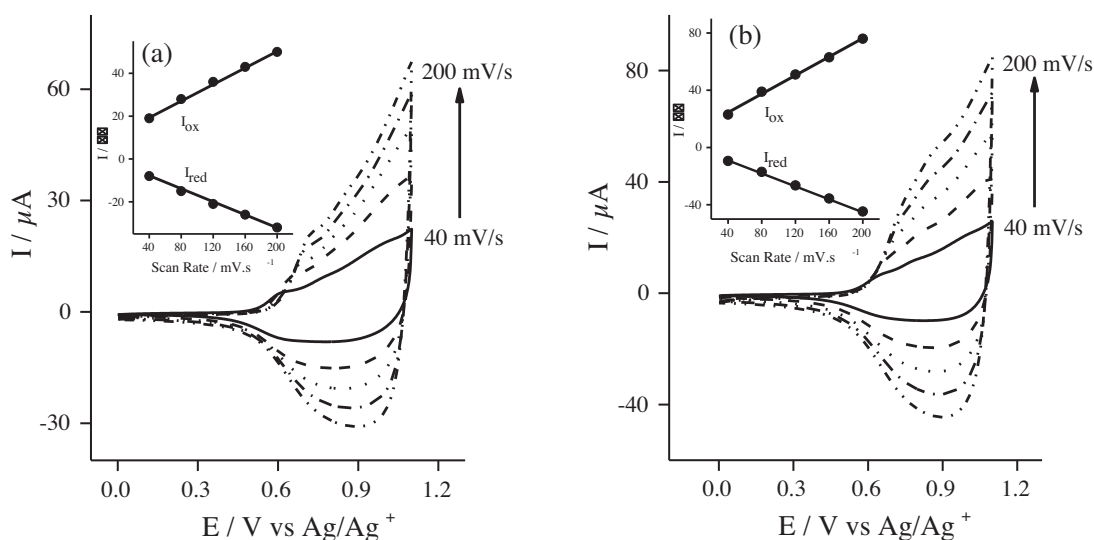


Figure 4. Cyclic voltammograms of the polymer films; a) **P(THBIMT)** and b) **P(TOBIMT)** with different scan rates up to 200 mV/s in 0.1 M TBABF₄/ACN. Insets: scan rate vs. anodic-cathodic current density graphs of the polymer films.

two absorption bands with the maximum peaks at 358 nm and 510 nm; the latter band is due to ICT (Figure 5b). During oxidation, the intensities of these bands decreased, which was accompanied by the appearance of a new intensifying band beyond 650 nm due to the formation of charge carriers. All spectra collected during oxidation of the polymers gave an isosbestic point at about 595 nm, indicating that the polymer films were interconverted between their neutral and oxidized states. Moreover, polymer films revealed the same electrochromic behavior in their neutral and oxidized states: from brick-red (L: 55, a: 25, b: 0.7 for **P(TOBIMT)**) to gray (L: 60, a: 4.1, b: -2.5 for **P(TOBIMT)**) upon oxidation (see insets of Figures 5a and 5b).

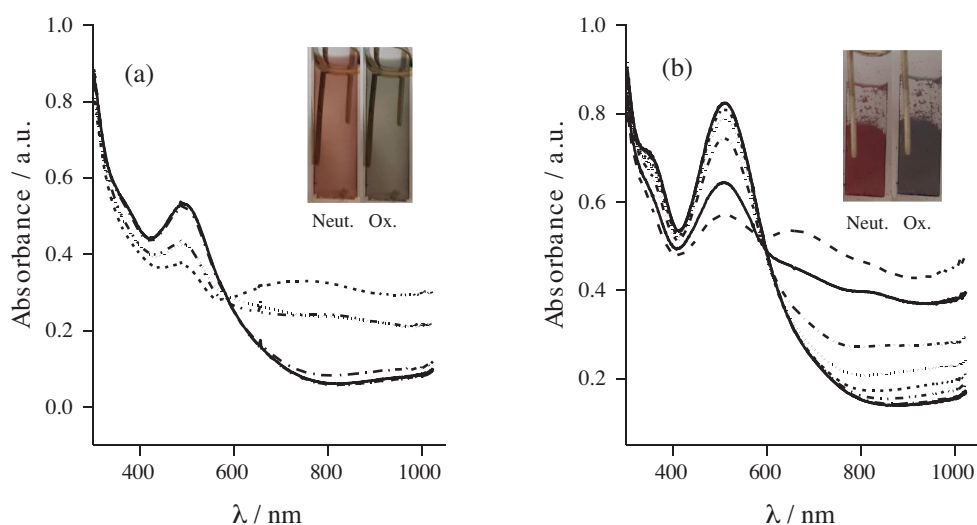


Figure 5. UV-Vis spectra of a) **P(THBIMT)** and b) **P(TOBIMT)** during the anodic scan via cyclic voltammetry (scan rate of 20 mV/s vs. Ag wire). Insets: colors of the polymer films in their neutral and oxidized states.

The optical band gap (E_g) was calculated from the onset of UV-Vis spectrum and found to be 1.62 eV for both polymers. Highest occupied molecular orbital (HOMO) and lowest unoccupied molecular orbital (LUMO) energy levels were calculated with respect to ferrocene (Fc^+/Fc), by using its energy level of 4.80 eV under vacuum,³¹ with the oxidation onset potential of 0.30 V vs. Ag/Ag^+ and the results are shown in Table 1.

Optical stability, percent transmittance (T %), switching times (t_{ox} and t_{red}), and coloration efficiency (CE) are important parameters for the optical characterization of conjugated polymers. To reveal these properties, a kinetic study was performed on the polymer films on the ITO-glass electrode, by applying 1.1 V and 0.0 V potentials every 5 s. The percent transmittance values for the polymer thin films were measured at 100% of the full contrast at the maximum of their ICT bands and are shown in Figure 6. **P(THBIMT)** gave 10% transmittance between its neutral (41%) and doped states (51%), and **P(TOBIMT)** showed 12% transmittance (15% to 27% upon oxidation). After 35 switches, percent transmittance of the **P(THBIMT)** decreased to 8%, a corresponding decrease of 20% in optical transparency. For **P(TOBIMT)**, T % was 8% after 50 switches, a corresponding decrease of 33%. As a result, the polymer films were found not to have good optical stability upon many switches between the full oxidation potential ranges. According to the kinetic spectra in Figures 6a and 6b, the oxidation and reduction times of the polymer films were 1.4 s and 1.2 s for **P(THBIMT)** and 1.6 s and 1.5 s for **P(TOBIMT)**, respectively.

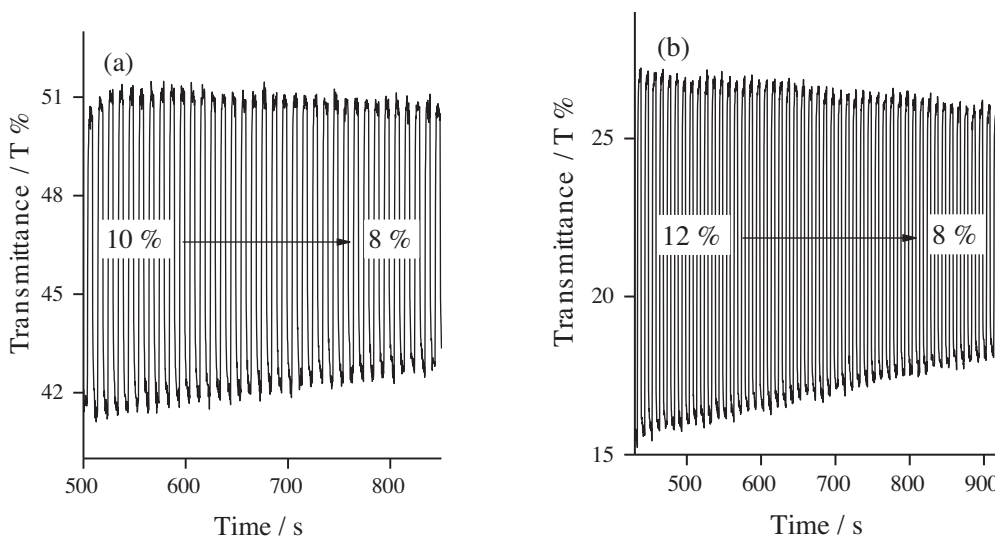


Figure 6. Percent transmittance change of a) **P(THBIMT)** at 504 nm and b) **P(TOBIMT)** at 510 nm, switched between their fully oxidized (1.1 V) and reduced (0.0 V) states with the residence time of 5 s.

CE shows the relation between optical absorbance change and charge–discharge density required for a full switch at a specific wavelength.³² CE is commonly measured and reported at 95% of the full optical contrast. For **P(THBIMT)** and **P(TOBIMT)**, CE values were calculated as 368 and 238 $\text{cm}^2 \text{C}^{-1}$, respectively, at 95% of the full optical contrast.³³ The optical properties of the polymers are summarized in Table 1.

According to above results, the electrochemical and optical properties of **P(THBIMT)** and **P(TOBIMT)** were the same. Both of the polymers can be obtained electrochemically as thin films on the working electrode. The polymer films are electroactive and can be doped and dedoped effectively, in reasonable potential ranges. The polymers have electrochromic behavior and change color from brick-red to gray upon oxidation. The thick-

Table 1. Electrochemical and spectrochemical properties of monomers and their polymer films.

	THBIMT	TOBIMT	P(THBIMT)	P(TOBIMT)
λ_{max}^a (nm)	300/487	300/487	360/504	358/510
E_{ox}^b (V)	1.02	1.02	0.92	0.92
E_{onset}^b (V)	0.90	0.90	0.45	0.45
E_g^a (eV)	2.19	2.19	1.62	1.62
HOMO	-5.72	-5.72	-4.95	-4.95
LUMO	-3.23	-3.23	-3.33	-3.33
T % ^c	-	-	10	12
CE ^c (cm ² C ⁻¹)	-	-	368	238
t_{ox}/t_{red}^c (s)	-	-	1.4/1.2	1.6/1.5

^aIn DCM for monomers, in TBABF₄/ACN for polymer films; ^bIn TBABF₄/ACN-DCM for monomers, in TBABF₄/ACN for polymer films; ^cAt corresponding low lying absorption bands of the polymer thin films (at 95% of the full contrast).

ness of the obtained film on ITO may change the coloration efficiency and percent transmittance, but not the optical band gap. On the other hand, the resulting polymers are insoluble in common organic solvents (DCM, chloroform, THF, dimethyl sulfoxide).

In order to investigate the acceptor unit effect, some other thiophene-containing polymers with different benzimidazole-based acceptor groups in the literature (Figure 7) were examined^{34–38} and the results are given in Table 2. Only the electrochemically obtained polymers were selected for better comparison.

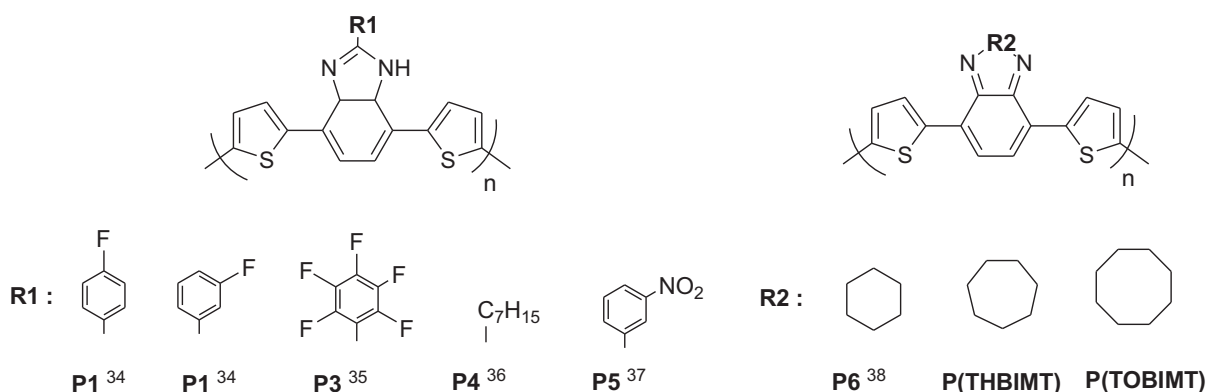


Figure 7. Electrochemically synthesized polymers including thiophene and BIM derivatives in the literature^{34–38} and in this study.

As shown in Figure 7, two types of benzimidazole derivatives can be prepared according to the substitution way. For example, BIMs in **P1**, **P2**, **P3**, **P4**, and **P5** are substituted one after their 2C and have band gaps in the range of 1.79–1.97 eV. On the other hand, BIMs in polymers **P6**, **P(THBIMT)**, and **P(TOBIMT)** are substituted directly at the 2C position and exhibit remarkably lower band gap values, within the range of 1.53–1.62 eV. It can be concluded that direct substitution of aromatic (or cyclic) groups on the 2C position

Table 2. Optical properties of the polymer films in Figure 7.

	λ_{max} (nm)	$E_g^{optical}$ (eV)	Electrolytic solution
P1 ³⁴	471	1.91	NaClO ₄ -LiClO ₄ /ACN
P2 ³⁴	440	1.96	NaClO ₄ -LiClO ₄ /ACN
P3 ³⁵	480	1.79	NaClO ₄ -LiClO ₄ /ACN
P4 ³⁶	440	1.93	NaClO ₄ -LiClO ₄ /ACN
P5 ³⁷	474	1.97	NaClO ₄ -LiClO ₄ /ACN
P6 ³⁸	389/575	1.53	TBAPF ₆ /ACN
P(THBIMT)	360/504	1.62	TBABF ₄ /ACN
P(TOBIMT)	358/510	1.62	TBABF ₄ /ACN

of benzimidazole causes a red shift in the optical absorption in the resulting polymers, with the corresponding decrease in the band gap.

Using the same electrolytic medium (sodium perchlorate (NaClO₄)–lithium perchlorate (LiClO₄) mixture in ACN) for characterization **P1**, **P2**, **P3**, **P4**, and **P5** allows making the comparison easier. Changing the F atom on the benzene ring of BIM from *meta*- (**P2**) to *para*- (**P1**) position causes a 31-nm red shift in the optical absorption, corresponding to a 0.05-eV decrease in the band gap. Similarly in **P5**, substituting the NO₂ unit at the *meta*- position results in a band gap of 1.97 eV, which is almost the same as that of **P2**. When all carbon atoms on benzene ring are fluorinated (**P3**), the band gap value decreases 0.12 eV more than that of **P1**. As a result, changing the position of substituting units on an aromatic ring at BIM affects the optical properties of resulting polymers.

P6 can be a good example for comparing with the polymers in this work. On the other hand, the electrolytic medium (tetrabutylammonium hexafluorophosphate (TBAPF₆) in ACN) used for polymer characterization is different. Moreover, the obtained polymer film is very thin, and the absorption intensity is very low.³⁸ Therefore, the band gap value is reported as 0.09 eV lower than **P(THBIMT)** and **P(TOBIMT)**, but the main electro-optical properties appear like those of the monomers in this study.

On the other hand, all of the electrochemically obtained conjugated polymers mentioned in Figure 7 are found to be insoluble, probably due to packaging tightly on the electrode surface.

In conclusion, benzimidazoles are exclusive acceptor units for band gap engineering, due to the ability of functionalization at the 2C position. Thus, various types of benzimidazole derivatives have been designed and used in the synthesis of DAD-type conjugated polymers.³⁹ In this study, new DAD-type conjugated monomers and their corresponding polymers were synthesized and electro-optical properties were revealed. Cycloheptyl- and cyclooctyl-substituted benzimidazole derivatives were used as the acceptor and thiophene was used as the donor. The polymer films were obtained electrochemically. Electrochemical and optical characterization of the polymers showed that both polymers can be doped and dedoped effectively and have an effective intramolecular charge transfer between the donor and the acceptor. Furthermore, changing the ring size on the benzimidazole has no appreciable effect on the properties of the resulting monomers and their corresponding polymers. When compared with other thiophene–benzimidazole-containing conjugated polymers in the literature, **P(THBIMT)** and **P(TOBIMT)** showed red-shifted optical absorption with the corresponding optical band gap values, indicating better conjugation in the polymer chain. Moreover, exhibiting good electrochemical stability and scan rate dependency makes these polymer films good candidates for electrochromic applications.

It is obvious that the benzimidazole unit can be substituted by different alkyl or cyclic-aromatic units and each resulting benzimidazole shows different electro-optical properties, even if they are coupled with the same donor.^{7,35,37,40} Thus, due to this main advantage, use of benzimidazole acceptors in donor-acceptor type of polymers will be continued in future studies.

3. Experimental

3.1. Materials and chemicals

All chemicals were purchased from Sigma Aldrich and used as received unless otherwise noted. Acetonitrile (ACN), dichloromethane (DCM), tetrahydrofuran (THF), and toluene were distilled and purged with nitrogen prior to use. Electrochemical studies were performed by using a platinum (Pt) disc as the working electrode, Pt wire as the counter electrode, and silver/silver chloride (Ag/Ag⁺) as the reference electrode. In the electrochemical synthesis of the polymers, 0.1 M tetrabutylammonium tetrafluoroborate (TBABF₄) dissolved in ACN-DCM (90:10 vol/vol) was used as the electrolytic medium. Electrochemical and spectroelectrochemical properties of the polymer films were investigated in 0.1 M TBABF₄-ACN electrolyte couple. The CVs were recorded with a Gamry potentiostat/galvanostat. An indium tin oxide (ITO, Delta Tech. 8-12, 0.7 cm × 5 cm) coated glass working electrode was used for obtaining the polymer films for spectrochemical studies. ¹H and ¹³C NMR spectra were recorded in deuteriochloroform (CDCl₃) on a Bruker Spectrospin Avance DPX-400 Spectrometer and chemical shifts were given relative to tetramethylsilane as the internal standard. The structures of the monomers were also confirmed by an Agilent (6224) model HRMS instrument. All of the measurements were performed at room temperature and in ambient conditions.

3.2. Synthesis

Before the synthesis of the monomers, the acceptor units were prepared according to a procedure described previously.⁴¹

General recipe for the synthesis of 4,7-dibromo-2-cycloheptyl-2H-benzo[d]imidazole or 4,7-dibromo-2-cyclooctyl-2H-benzo[d]imidazole: 3,6-dibromobenzene-1,2-diamine (1 eq), cycloheptanone or cyclooctanone (3.7 eq), and acetic acid (0.1 eq) are mixed and refluxed in diethyl ether under inert atmosphere with continuous stirring. The reaction is followed by TLC. At the end of the reaction, the solvent is removed and the organic phase is collected by washing with ethyl acetate and saturated aqueous brine. The crude product is purified over column chromatography (20:1 hexane:ethyl acetate). The obtained yellowish oil is stirred with activated MnO₂ (3 eq) in freshly distilled THF overnight. The reaction mixture is then filtered, washed with THF, and the final product is obtained as yellow needles after purifying via column chromatography (15:1 hexane:ethyl acetate). ¹H NMR (400 MHz, CDCl₃) δ (ppm): 7.17 (s, 2H); 1.7-1.71 (m, 14H); ¹³C NMR (100 MHz, CDCl₃) δ (ppm): 156.8; 135.7; 118.9; 110.8; 77.2; 41.9; 27.2; 22.7.

Synthesis of the monomers; 4,7-di-2-thienylspiro[benzimidazole-2,1'-cycloheptane] (**THBIMT**) and 4,7-di-2-thienylspiro[benzimidazole-2,1'-cyclooctane] (**TOBIMT**): The monomer synthesis was achieved according to the general procedure of Stille coupling reaction; 4,7-dibromo-2-cycloheptyl-2H-benzo[d]imidazole (or 4,7-dibromo-2-cyclooctyl-2H-benzo[d]imidazole) (1 eq), tributyl(thiophen-2-yl)stannane (2.1 eq), and Pd(II) (2% eq) are dissolved in freshly distilled toluene and refluxed for approximately 2 days under inert atmosphere. After evaporation of toluene, the crude product is dissolved in DCM and washed with saturated aqueous solution of sodium chloride. The collected organic phase is dried over MgSO₄ and purified via column chromatography (4:1

hexane: DCM) to obtain dark orange solid. **THBIMT**: ^1H NMR (400 MHz, CDCl_3) δ (ppm): 7.71 (dd, 2H), 7.50 (d, 2H), 7.38 (d, 2H), 7.12 (m, 2H), 0.80–2.10 (m, 12H). HRMS (m/z): calcd for $\text{C}_{21}\text{H}_{20}\text{N}_2\text{S}_2$, 364.1068; found, 365.1175 [M + H].⁺ **TOBIMT**: ^1H NMR (400 MHz, CDCl_3) δ (ppm): 7.98 (dd, 2H), 7.42 (d, 2H), 7.29 (d, 2H), 7.05 (m, 2H), 0.80–2.10 (m, 14H). HRMS (m/z): calcd for $\text{C}_{22}\text{H}_{22}\text{N}_2\text{S}_2$, 378.1224; found, 379.1342 [M + H].⁺

Acknowledgment

I would like to thank to Prof Dr Ahmet M Onal (from Middle East Technical University, Turkey) for sharing his laboratory equipment and chemicals, as well as providing the best academic support.

References

1. Farges, J. P. *Organic Conductors: Fundamentals and Applications*; Marcel Dekker: New York, NY, USA, 1994.
2. Feast, W. J.; Tsibouklis, J. K.; Pouwer, L.; Groenendaal, L.; Meijer, E. W. *Polymer* **1996**, *37*, 5017-5047.
3. Nalwa, H. S. *Handbook of Organic Conductive Molecules and Polymers*; Wiley: Chichester, UK, 1997.
4. Roncali, J. *Chem. Rev.* **1997**, *97*, 173-206.
5. Barbarella, G.; Favaretto, L.; Sotgiu, G.; Zambianchi, M.; Arbizzani, C.; Bongini, A.; Mastragostino, M. *Chem. Mater.* **1999**, *11*, 2533-2541.
6. Arbizzani, C.; Mastragostino, M.; Soavi, F. *Electrochim. Acta* **2000**, *45*, 2273-2278.
7. Nurulla, I.; Morikita, T.; Fukumoto, H.; Yamamoto, T. *Macromol. Chem. Phys.* **2001**, *202*, 2335-2340.
8. Wang, M.; Hu, X.; Liu, P.; Li, W.; Gong, X.; Huang, F.; Cao, Y. *J. Am. Chem. Soc.* **2011**, *133*, 25, 9638-9641.
9. Tonzola, C. J.; Alam, M. M.; Bean, B. A.; Jenekhe, S. A. *Macromolecules* **2004**, *37*, 3554-3563.
10. Froehlich, J. D.; Young, R.; Nakamura, T.; Ohmori, Y.; Li, S.; Mochizuk, A. *Chem. Mater.* **2007**, *19*, 4991-4997.
11. Rauh, R. *Electrochim. Acta* **1999**, *44*, 3165-3176.
12. Brabec, C. J.; Sariciftci, N. S.; Hummelen, J. C. *Adv. Funct. Mater.* **2001**, *11*, 15-26.
13. Coakley, K.; McGehee, M. D. *Chem. Mater.* **2004**, *16*, 4533-4542.
14. Hong, Y.; Wong, H.; Moh, L. C. H.; Tan, H.; Chen, Z. *Chem. Commun.* **2011**, *47*, 4920-4922.
15. Yang, C.; Kim, J. Y.; Cho, S.; Lee, J. K.; Heeger, A. J.; Wudl, F. *J. Am. Chem. Soc.* **2008**, *130*, 6444-6450.
16. Mortimer, R. J.; Dyer, A. L.; Reynolds, J. R. *Display* **2006**, *27*, 2-18.
17. Beaupré, S.; Breton, A. C.; Dumas, J.; Leclerc, M. *Chem. Mater.* **2009**, *21*, 1504-1513.
18. Gerard, M.; Chaubey, A.; Malhotra, B. D. *Biosensors and Bioelectronics* **2002**, *17*, 345-359.
19. Kutkan, S.; Goker, S.; Hacıoglu, S. O.; Toppare, L. J. *Macromol. Sci. Part A* **2016**, *53*, 8, 475-483.
20. Nie, W.; MacNeill, C. M.; Li, Y.; Nofle, R. E.; Carroll, D. L.; Coffin, R. C. *Macromol. Rapid Commun.* **2011**, *32*, 1163-1168.
21. Zhang, L. J.; He, C.; Chen, J. W.; Yuan, P.; Huang, L. A.; Zhang, C.; Cai, W. Z.; Liu, Z. T.; Cao, Y. *Macromolecules* **2010**, *43*, 9771-9778.
22. Li, J. C.; Lee, H. Y.; Lee, S. H.; Zong, K.; Jin, S. H.; Lee, Y. S. *Synth. Met.* **2009**, *159*, 201-208.
23. Sonar, P.; Singh, S. P.; Leclère, P.; Surin, M.; Lazzaroni, R.; Lin, T. T.; Dodabalapur, A.; Sellinger, A. *J. Mater. Chem.* **2009**, *19*, 3228-3237.
24. Cansu-Ergun, E. G.; Akbayrak, M.; Akdag, A.; Onal, A. M. *J. Electrochem. Soc.* **2016**, *163*, 10, G153-G158.

25. Nurulla, I.; Tanimoto, A.; Shiraishi, K.; Sasaki, S.; Yamamoto, T. *Polymer* **2002**, *43*, 1287-1293.
26. Song, S.; Jin, Y.; Park, S. H.; Cho, S.; Kim, I.; Lee, K.; Heeger, A. J.; Suh, H. J. *Mater. Chem.* **2010**, *20*, 6517-6523.
27. Ozelcaglayan, A. C.; Sendur, M.; Akbasoglu, N.; Apaydin, D. H.; Cirpan, A.; Toppare, L. *Electrochim. Acta* **2012**, *67*, 224-229.
28. Cansu-Ergun, E. G.; Önal, A. M.; Cihaner, A. *J. Electrochem. Soc.* **2016**, *163*, 5, G53-G60.
29. Zaifoglu, B.; Sendura, M.; Akbasoglu Unlu, N.; Toppare, L. *Electrochim. Acta* **2012**, *85*, 78-83.
30. Gibson, G. L.; McCormick, T. M.; Seferos, D. S. *J. Am. Chem. Soc.* **2012**, *134*, 539-547.
31. Deng, P.; Liu, L.; Ren, S.; Li, H.; Zhang, Q. *Chem. Commun.* **2012**, *48*, 6960-6962.
32. Beaujuge, P. M.; Reynolds, J. R. *Chem. Rev.* **2010**, *110*, 1, 268-320.
33. Bechinger, C.; Burdis, M. S.; Zhang, J. G. *Solid State Commun.* **1997**, *101*, 753-756.
34. Ileri, M.; Hacioglu, S. O.; Toppare, L. *Electrochim. Acta* **2013**, *109*, 214-220.
35. Ileri, M.; Hacioglu, S. O.; Cirpan, A.; Toppare, L. *J. Macromol. Sci. Pure* **2015**, *52*, 510-516.
36. Nurioglu, A. G.; Akpınar, H.; Sendur, M.; Toppare, L. *J. Polym. Sci. Pol. Chem.* **2012**, *50*, 3499-3506.
37. Soylemez, S.; Hacioglu, S. O.; Demirci Uzun, S.; Toppare, L. *J. Electrochem. Soc.* **2015**, *162*, H6-H14.
38. Al-Ogaidi, S.; Karabay, B.; Karabay, L. C.; Cihaner, A. *J. Electroanal. Chem.* **2018**, *58*, 42-62.
39. Cansu Ergun, E. G. *Pol. Rev.* **2018**, *58*, 42-62.
40. Akpınar, H.; Balan, A.; Baran, D.; Unver, E. K.; Toppare, L. *Polymer* **2010**, *51*, 6123-6131.
41. Cansu-Ergun, E. G.; Onal, A. M.; Cihaner, A. *Electrochim. Acta* **2016**, *188*, 165-174.